Advanced Engineering Forum
ISSN: 2234-991X, Vols. 2-3, pp 942-947
doi:10.4028/www.scientific.net/AEF.2-3.942

Online: 2011-12-22

The Gyroscopic Effect on Dynamic Characteristics of Dual- Disk Rotor System

Meiling Wang[a], Qingkai Han*

School of Mechanical Engineering & Automation, Northeastern University, Shenyang, China

[a] meilingcc@163.com * qhan@mail.neu.edu.cn (corresponding author)

Keywords: gyroscopic effect, dual-disk rotor system, critical speed, unbalances response

Abstract. Although the gyroscopic effect on rotor system has been noticed for decades, it is often underestimated and even ignored in the simplified model; moreover the comparing analyses of it on dynamics of rotor system with distributed masses are rarely performed. In this paper, a model of dual-disk rotor system with 8 degree-of-freedoms is developed to show the gyroscopic effects, especially on asymmetric rotor system, in which the polar and transversal moments of inertia of the disks are incorporated. The critical speeds and unbalance responses of such a rotor system are simulated numerically and compared respectively in 4 different asymmetric cases, including 2 cases of position asymmetry and another 2 cases of support stiffness asymmetry. The analysis results clearly show that the gyroscopic effect has obvious influence on the critical speeds and unbalance responses under different asymmetry conditions.

Introduction

Dynamics research and vibration analysis of rotor system commonly used in rotating machine are very useful. The lateral transversal vibrations of rotor system are most popular, while rotor lateral angular motion is also very important, as it introduces a new phenomenon in the rotor behavior, namely the gyroscopic effect [1].

The gyroscopic effect, as related to rotor dynamics, has been notoiced for decades, starting from pioneering works by Smith (1933), Yamamoto (1954), Dimentberg (1961)[2-4], considering various ways of unfolding the rotor lateral transversal and angular motion. In 1986, Muijderman[5] investigated the interaction between the stabilizing effect of gyroscopic moment and destabilizing effect of fluid-induced tangential forces. Descriptions of gyroscopic effects in detail can be found in the publications by Vance (1988)[6]. Gyroscopic effect has been incorporated in the dynamic analysis of rotor shaft system [7].Although the gyroscopic effect plays a significant role in rotor dynamics [8] and has been researched for decades; the impact analysis for gyroscopic effect has been rarely performed. Moreover, the gyroscopic effect is often underestimated and even ignored in the simplified rotor system model.

In this paper, a simplified model for a dual-disk rotor system with 8 degree of freedom is developed to show the gyroscopic effects, in which the polar and transversal moments of inertia of the disks are incorporated. The critical speeds and unbalance responses of such a rotor system are simulated numerically and compared respectively in 4 different asymmetric cases, including 2 cases of position asymmetry and another 2 cases of support stiffness asymmetry.

Model of the dual-disk rotor system

Equations of motion. In order to study the gyroscopic effect, a simplified dual-disc rotor system model is developed. The system is illustrated in Fig. 1, and it consists of one flexible shaft, two rigid disks and two elastic bearing supports. The axial, flexural and torsional behaviors of rotor system are uncoupled, and one disk with 4 degrees of freedom is adequate for the study of the flexural behavior [8], so the model for the dual-disk rotor system with 8 degree of freedom is adopted in this paper shown in Fig. 1(a).

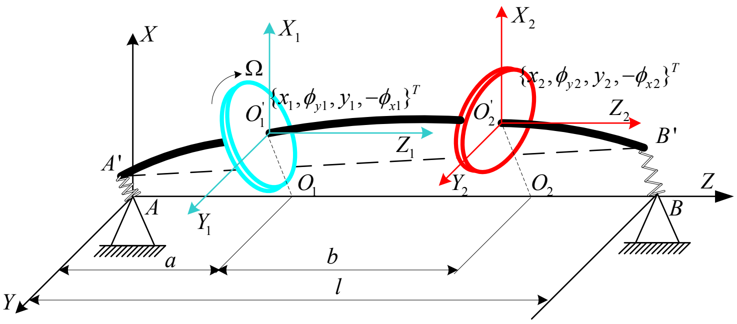

(a)Diagram of a dual-disk rotor system with 8 degree of freedom

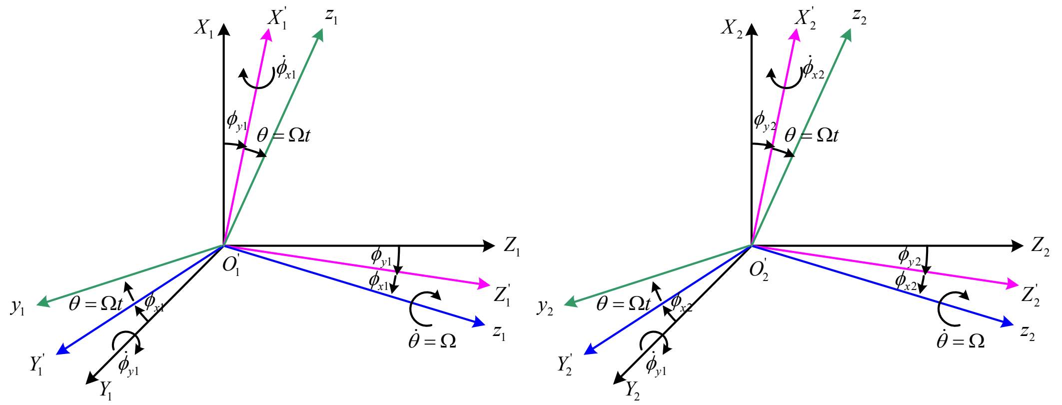

(b) Reference frame of the first disk (c) Reference frame of the second disk

Fig. 1. Diagram of dual disks rotor system and two reference frames origin in $O_1^{'}$, $O_2^{'}$ respectively

The global fixed frame is set as *AXYZ*, origin in A, one of the support points, *Z*-axis of which coinciding with the rotation axis of the rotor. The reference frame $O_1^{'}X_1Y_1Z_1$ of the first disk, origin in $O_1^{'}$, the center of the first disk, is the space-fixed frame and parallel with the global fixed frame. After rotations (1) ϕ_{y1} about Y_1 (2) ϕ_{x1} about $X_1^{'}$ (3) $\theta = \Omega t$ about z_1 (where Ω is the rotating speed), the body-fixed principal frame of the first disk $O_1^{'}x_1y_1z_1$ is obtained, shown in Fig. 1(b). The reference frame of the second disk $O_2^{'}x_2y_2z_2$ can be obtained in the same way, shown in Fig. 1(c).

The equations of motion of the rotor are derivable from the potential and kinetic energy functions by using Lagrange's equation. The detail derivations are described in the reference [8] and the final equations are

$$\begin{aligned} &\boldsymbol{M}\ddot{\boldsymbol{X}} + \Omega\boldsymbol{J}\dot{\boldsymbol{Y}} + \boldsymbol{C}\dot{\boldsymbol{X}} + \boldsymbol{K}_{xz}\boldsymbol{X} = \boldsymbol{Q}_{xz} \\ &\boldsymbol{M}\ddot{\boldsymbol{Y}} - \Omega\boldsymbol{J}\dot{\boldsymbol{X}} + \boldsymbol{C}\dot{\boldsymbol{Y}} + \boldsymbol{K}_{yz}\boldsymbol{Y} = \boldsymbol{Q}_{xz} \end{aligned} \tag{1}$$

where $\boldsymbol{X} = \{x_1 \quad \phi_{y1} \quad x_2 \quad \phi_{y2}\}^T$, $\boldsymbol{Y} = \{y_1 \quad -\phi_{x1} \quad y_2 \quad -\phi_{x2}\}^T$ are the generalized displacement vectors of the rotor system; x_1, y_1 are the transverse displacement components of the first disk center; x_2, y_2 are the transverse displacement components of the second disk center; $\phi_{y1}, \phi_{x1}, \phi_{y2}, \phi_{x2}$ are the rotating angle displacements of the two disk, respectively. $\boldsymbol{M}$, $\boldsymbol{J}$, $\boldsymbol{C}$, $\boldsymbol{K}_{xz}$, $\boldsymbol{K}_{yz}$ are the mass matrix, gyroscopic matrix, damping matrix, and stiffness matrixes in *XZ*- and *YZ*-plane, respectively. The stiffness matrix can be obtained by inverting the compliance matrix [8]. The matrices of $\boldsymbol{M}$, $\boldsymbol{J}$ are

$$\boldsymbol{M} = \begin{bmatrix} m_1 & & & 0 \\ & J_{t1} & & \\ & & m_2 & \\ 0 & & & J_{t2} \end{bmatrix}, \boldsymbol{J} = \begin{bmatrix} 0 & & & 0 \\ & J_{p1} & & \\ & & 0 & \\ 0 & & & J_{p2} \end{bmatrix} \tag{2}$$

where, m_1, m_2 are the masses of the two disks; J_{t1}, J_{t2} are the transverse moments of inertia of the two disks about any axis in its own rotation plane; J_{p1}, J_{p2} are the polar moments of inertia of the two disks about the rotation axis.

The external force vectors $\boldsymbol{Q}_{xz}, \boldsymbol{Q}_{yz}$ along X- and Y- directions include the unavoidable unbalances of the disks. They are expressed as follows,

$$\begin{aligned} \boldsymbol{Q}_{xz} &= \{m_1 e_1 \Omega^2 \cos(\Omega t + \alpha_1) \quad 0 \quad m_2 e_2 \Omega^2 \cos(\Omega t + \alpha_2) \quad 0\}^T \\ \boldsymbol{Q}_{yz} &= \{m_1 e_1 \Omega^2 \sin(\Omega t + \alpha_1) \quad 0 \quad m_2 e_2 \Omega^2 \sin(\Omega t + \alpha_2) \quad 0\}^T \end{aligned} \tag{3}$$

where, $m_1 e_1 \Omega^2 \cos(\Omega t + \alpha_1)$ and $m_1 e_1 \Omega^2 \sin(\Omega t + \alpha_1)$ are the unbalanced forces of the first disk in the X- and Y- directions with eccentricity e_1 and initial phases α_1 respectively. And correspondingly, $m_2 e_2 \Omega^2 \cos(\Omega t + \alpha_2)$ and $m_2 e_2 \Omega^2 \sin(\Omega t + \alpha_2)$ are the unbalanced forces of the second disk with eccentricity e_2 and initial phases α_2 along X- and Y- directions.

Critical speeds of the dual-disk rotor system. In the analysis of the dual rotor system critical speeds, the assumptions are as follows. It is acceptable to assume that $\boldsymbol{K}_{xz} = \boldsymbol{K}_{yz} = \boldsymbol{K}$, because the situation in the XZ- plane is similar to that in the YZ-plane. The damped effect is not considered for the rotor system, i.e., $\boldsymbol{C}$ is taken as zero in the motion equations, and the external forces are not included either.

Introducing the complex coordinates $\boldsymbol{q} = \boldsymbol{X} + i\boldsymbol{Y}$ in the homogeneous equations associated with Equations (1) with the above assumptions, the equation of motion is reduced to

$$\boldsymbol{M}\ddot{\boldsymbol{q}} - i\Omega \boldsymbol{J}\dot{\boldsymbol{q}} + \boldsymbol{K}\boldsymbol{q} = \boldsymbol{0} \tag{4}$$

Then introducing a solution of the type $\boldsymbol{q} = \boldsymbol{q}_0 e^{i\omega t}$ into the reduced equation, the following algebraic linear equation is readily obtained:

$$(-\boldsymbol{M}\omega^2 + \boldsymbol{J}\Omega\omega + \boldsymbol{K})\boldsymbol{q}_0 = \boldsymbol{0} \tag{5}$$

where ω is the whirl frequency. The characteristic equation allowing computation of the whirl frequency is

$$\left| -\boldsymbol{M}\omega^2 + \boldsymbol{J}\Omega\omega + \boldsymbol{K} \right| = 0 \tag{6}$$

Equation (6) has 8 real roots, 4 of which are positive, corresponding to the forward whirl, and the other 4 roots related to the backward whirl are negative.

Gyroscopic effects on the dual-disk rotor system

To analyze the gyroscopic effect on the dual-disk rotor system and compare the effect on the critical speed and unbalance response of the system under different asymmetric conditions, the eigenvalues of the undamped dual-disk rotor system are calculated by solving the characteristic equation (6), and the numerical integration of Esq. (1) is also carried out by using Runge-Kutta method. The initial parameters selected in the model are as follows. Both of the masses of two disks are 1Kg with diameter 200mm, and the shaft with an elastic modulus of 2.06×10^{11}Pa is 12 mm in diameter and 450mm in length. The distance between the first disk and the support point A is a=150 mm. The second disk is located in symmetry, and the distance between the two disks is b=150 mm. The support stiffness at two points is set as to $K_A = K_B = 1.0\times10^8$ N/m.

For comparing the gyroscopic effect under different asymmetric conditions, the parameters used in the following 4 asymmetric cases are here based on the initial parameters.

Case (a): The distance between the first disk and the support point A and the one between the two disks are all altered from 150 mm to 100 mm, i.e., a=b=100 mm.

Case (b): The distance between the first disk and the support point A and the one between the two disks are all changed to 80 mm, i.e., $a=b=80$ mm.

Case (c): The support stiffness at the point B is set as to $K_B = 1.0\times10^6$ N/m instead.

Case (d): The support stiffness at the point B is converted to $K_B = 1.0\times10^4$ N/m.

Gyroscopic effects on the critical speeds. In order to compare gyroscopic effect on the critical speed of the undamped rotor system with two disks, four asymmetry cases mentioned above are considered. Case (a) and (b) will be referred to as position asymmetry which in case (b) is greater than that in case (a). Besides, case(c) and (d) will be as the support stiffness asymmetry, and the latter is more asymmetric than the former. The Campbell diagrams of the system in the 4 asymmetric cases mentioned above are illustrated in Fig. 2(a)~(d), in which 'B' denotes backward whirl, and 'F' forward whirl, and the dotted line $\omega = \Omega$ is drawn at an angle of 45° to the x-axis.

The Campbell diagrams of Fig. 2(a)~(d) are corresponding to the 4 asymmetric cases (a)~(d), from which it can be seen that as the rotating speed increases, the stiffening due to gyroscopic effect increases and the eigenvalues for the forward whirl increases and for the backward whirl decreases. Moreover, the more asymmetric the rotor system is, the more obvious differences due to the gyroscopic effect are.

Whenever the rotating speed coincides with any of the eigenvalues, resonance occurs and thus we can confirm the critical speeds at the points of intersection between the dotted line and the plots of eigenvalues. In each of the Campbell diagrams shown in Fig. 2, two intersection points give the first two order critical speed, and the other two can not be obtained as the rotating speed increasing. The first two order critical speed for the 4 asymmetric cases are compared and listed in Table 1.

Table1 Gyroscopic effect on the critical speed in 4 asymmetric cases

Variable	Order	SNG /Hz	FSWG/Hz	DR
Case(a) $a=b=100$ mm	First	43.4371	45.7344	5.29%
	Second	186.8171	298.5839	59.83%
Case(b) $a=b=80$ mm	First	47.0434	51.5243	9.53%
	Second	208.3776	433.8334	108.20%
Case(c) $K_B=1.0\times10^6$N/m	First	41.8657	43.4511	3.79%
	Second	152.0841	172.3656	13.34%
Case(d) $K_B=1.0\times10^4$N/m	First	36.4679	37.3763	2.49%
	Second	123.7397	154.6155	24.95%

***Note**: SNG-critical speed without gyroscopic effect; FSWG-forward whirl critical speed with gyroscopic effect; DR-deviation rate between the SNG and FSWG

From Table 1, it is clearly seen that the gyroscopic effect on the critical speed is obvious. When the position and support stiffness asymmetry existing, the first order critical speed of the dual-disk rotor system with gyroscopic effect is little higher than that without the gyroscopic effect, but the second order critical speed is much higher than that without gyroscopic effect. In addition, the gyroscopic effect is more obvious in the greater asymmetry cases (b) and (d) than that in the cases (a) and (c).

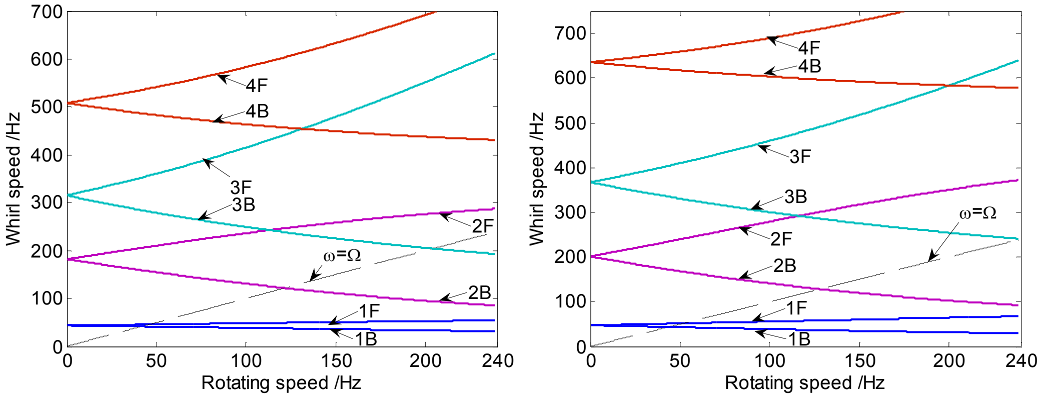

(a)When a=b=100 mm (b) When a=b=80 mm

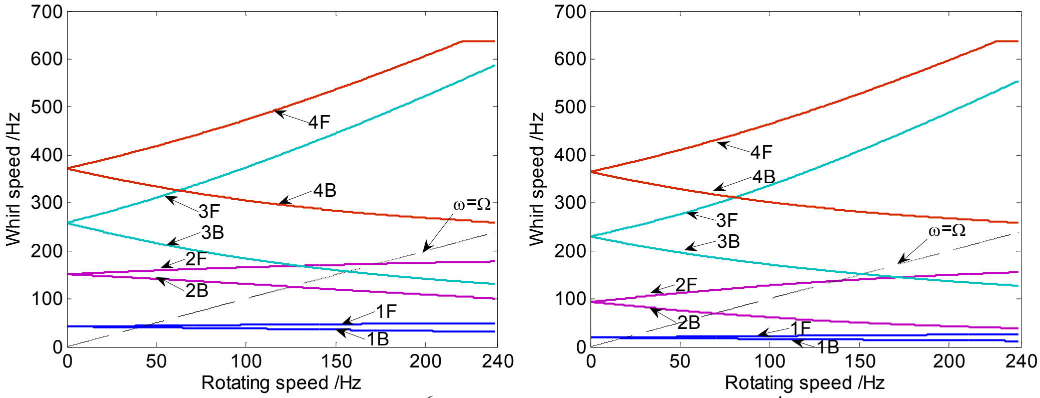

(c) When K_B=1.0×10^6 N/m (d) When K_B=1.0×10^4 N/m

Fig. 2. Campbell diagram in 4 asymmetric cases

Gyroscopic effects on unbalance responses. The simulations are carried out by numerical integration of Esq. (1) by using Runge-Kutta method to analyze the gyroscopic effects on the unbalance responses. In the numerical simulation for the unbalance responses of the rotating disks, the unbalances of the two disks are set as to 300g.mm, and the rotating speed of the rotor varies from about 30Hz to 150Hz, and the other parameters are the same as for Fig. 2. Four different asymmetric cases are calculated respectively. The obtained unbalance responses amplitudes of the first disk along the rotating speed are illustrated in Fig. 3.

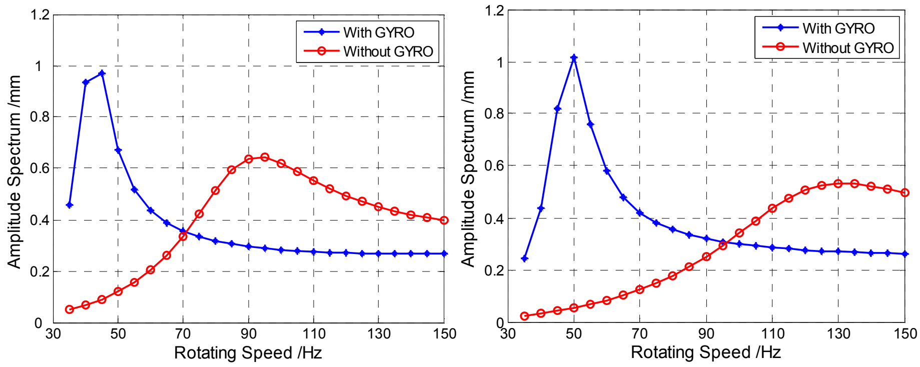

(a)When a=b=100 mm (b) When a=b=80 mm

Figures 3(a)~(d) are corresponding to the cases (a)~(d) respectively, in which 'with GYRO' and 'without GYRO' denote with and without consideration of the gyroscopic effect respectively. From Fig. 3 it can be clearly seen that the unbalance response amplitudes with and without consideration of the gyroscopic effect are not equal at the same rotating speed and their peaks are not coinciding with each other. And predominantly due to the gyroscopic effect, the amplitudes are smaller that that without gyroscopic effect, when the rotating speed exceeding a certain speed. Gyroscopic effect plays an important role in the unbalance response, and the role is more obvious as the position asymmetry and support stiffness asymmetry become greater.

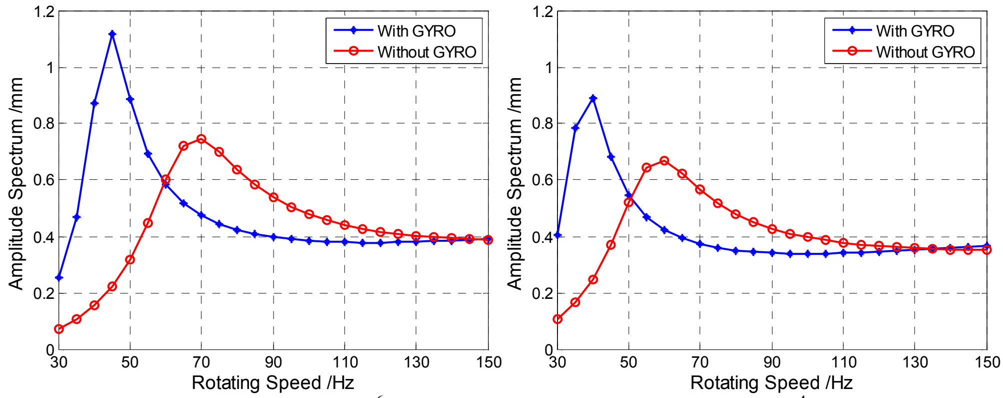

(c) When K_B =1.0×10^6 N/m (d) When K_B =1.0×10^4 N/m

Fig. 3. Diagram of unbalance response amplitudes of the first disk along the rotating speed

Results and conclusions

The model of a dual-disk rotor system is established, in which the corresponding gyroscopic effects are considered. The gyroscopic effect on the critical speed and unbalance responses of the rotor system are investigated in the conditions of position asymmetry and the support stiffness asymmetry. The following conclusions are drawn.

(1) As the rotating speed increases, the eigenvalues for the forward whirl increases and for the backward whirl decreases due to gyroscopic effect. The first order critical speed of the dual-disk rotor system with gyroscopic effect is little higher than that without the gyroscopic effect, but the second order critical speed is much higher than that without gyroscopic effect. In addition, the gyroscopic effect is more obvious in the greater asymmetry.

(2)The gyroscopic effect plays an important role in the unbalance response under the position asymmetry and support stiffness asymmetry conditions. And the role is more obvious as the asymmetry become greater. So, it is not reasonable to ignore the gyroscopic effect of the dual-disk rotor system.

Acknowledgements

This work was financially supported by the Natural Science Foundation of China (Grant No: 51175070), and Fundamental Research Funds for the Central Universities (N090603007).

References

[1] Muszyska A. Rotordynamics. Taylor & Francis Group, 2005
[2] Smith, D.M., The motion of a rotor carried by a flexible shaft in flexible bearings, Proc. Roy. Soc. (A) 142 (1933), 92
[3] Yamamoto, T., On the Critical Speeds of a Shaft, Memoirs of the Faculty of Engineering, Nagoya University, 1954.
[4] Dimentberg, F.M., Flexural Vibrations of Rotating Shaft, London: Butterworths, 1961.
[5] Muijderman, E.A., Algebraic formulas for the threshold and mode of instability and the first critical speed of a simple flexibly supported (overhung) rotor-bearing system, Proceedings of the International Conference on Rotor dynamics, Tokyo, Japan, 1986, pp. 201
[6] Vance J M, Rotordynamics of Turbomachinery. A Wiley-Interscience Publication, 1988
[7] Dutt J K, Nakra B C, Dynamics of rotor shaft system on flexible supports with gyroscopic effects, Mechanics Research Communications, 22(1995) 541-545
[8] Genta G, Dynamics of Rotating Systems, Springer, 2005